Analytical and Bioanalytical Chemistry
https://doi.org/10.1007/s00216-017-0786-8

RESEARCH PAPER

An aptamer-based biosensor for detection of doxorubicin by electrochemical impedance spectroscopy

Nicole Bahner[1] · Peggy Reich[1] · Dieter Frense[1] · Marcus Menger[2] · Katharina Schieke[1] · Dieter Beckmann[1]

Received: 31 August 2017 / Revised: 31 October 2017 / Accepted: 24 November 2017

Abstract

An aptamer-based biosensor was developed for the detection of doxorubicin using electrochemical impedance spectroscopy. Doxorubicin and its 14-dehydroxylated version daunorubicin are anthracyclines often used in cancer treatment. Due to their mutagenic and cardiotoxic effects, detection in groundwater is desirable. We developed a biosensor using the daunorubicin-binding aptamer as biological recognition element. The aptamer was successfully co-immobilized with mercaptohexanol on gold and a density of $1.3*10^{13} \pm 2.4*10^{12}$ aptamer molecules per cm^2 was achieved. The binding of doxorubicin to the immobilized aptamer was detected by electrochemical impedance spectroscopy. The principle is based on the inhibition of electron transfer between electrode and ferro-/ferricyanide in solution caused by the binding of doxorubicin to the immobilized aptamer. A linear relationship between the charge transfer resistance (R_{ct}) and the doxorubicin concentration was obtained over the range of 31 nM to 125 nM doxorubicin, with an apparent binding constant of 64 nM and a detection limit of 28 nM. With the advantages of high sensitivity, selectivity, and simple sensor construction, this method shows a high potential of impedimetric aptasensors in environmental monitoring.

Keywords Aptasensor · Faradaic EIS · Electroanalytical methods · Water pollution · Self-assembly

Introduction

Doxorubicin and its 14-dehydroxylated version daunorubicin belong to the group of anthracycline antibiotics and are used as chemotherapeutic agents in cancer therapy [1]. Animal experiments have shown that doxorubicin is mutagenic, cardio- and embryotoxic. The median lethal dose LD_{50} of doxorubicin if administered orally is for mice 205 mg/kg and for rats 336 mg/kg. For humans the lowest lethal dose known if administered orally is 6 mg/kg [2]. Due to its toxic effect on proliferating cells, strong side effects such as hair loss, vomiting, bone marrow depression, and cardiotoxicity can occur during chemotherapy [3]. During medical treatment, this drug reaches the sewage system. Mahnik et al. investigated the sewage of an oncological station at Vienna General Hospital over a period of 2 y and detected doxorubicin in the range from 0.48 to 2.48 nM [4]. Owing to incomplete degradation in sewage treatment plant, it gets into the ground- and drinking water. It contaminates nature and endangers humans and the environment in high concentrations because of its cardiotoxicity.

So far, the detection of doxorubicin has been carried out using various classic analytical methods such as gas chromatography [5, 6], liquid chromatography [7], high-performance liquid chromatography [8, 9], UV-Vis spectroscopy [10], fluorescence spectroscopy [11, 12], and capillary electrophoresis [13, 14]. Using these classic methods, concentrations in the nanomolar range could be detected (down to 1 nM). However, these methods require a high instrumental effort and can only be handled by qualified people. Erdem et al. developed a voltammetric and impedimetric graphite sensor against daunorubicin based on dendrimers and was able to reach a detection limit of 128 nM [15].

An alternative to dendrimers as biological recognition element are aptamers. These play an increasingly important role

Parts of this work were presented at the First European / 10th German BioSensor Symposium, Potsdam, 2017.

✉ Nicole Bahner
N.Bahner@hs-mannheim.de

[1] Institute for Bioprocess and Analytical Measurement Technology e.V. Rosenhof, 37308 Heilbad Heiligenstadt, Germany

[2] Fraunhofer Institute for Cell Therapy and Immunology, Branch Bioanalytics and Bioprocesses (IZI-BB), Am Mühlenberg 13, 14476 Potsdam, Germany

Published online: 03 December 2017

in the development of biosensors. Aptamers are artificial single-stranded nucleic acids with typical molecular lengths of 15 to 150 nucleotides; they bind their targets by their specific three-dimensional structure. Once selected, aptamers are chemically synthesized, which is not only cost-effective but also provides consistent quality and enables chemical modifications as, e.g., to improve stability or introduce functional groups, which favor the wide range of applications.

A large number of aptamers for pharmaceuticals were developed, e.g., hormones, antibiotics, and psychotropic substances [16]. Most drugs are small molecules with a molecular weight <900 daltons. The detection of aptamer binding with small target molecules implicates some difficulties since the molecular weight is low and certain aptamer–target interactions (e.g., hydrogen bonds and electrostatic interactions) are greatly reduced due to the simple structures [17], which influences the binding strength and hence the stability of the measurement signal. Therefore most aptasensors for small molecules are based on optical or electrochemical measurement methods. One small molecule detected by an aptamer is the mutagenic and carcinogenic ethanolamine (M = 61.08 g/mol) [18]. Liang et al. (2016) described an impedimetric aptasensor for ethanolamine with a detection limit of 0.08 nM [19]. Other small molecules detected by electrochemical measurement methods were cocaine [20], aminoglycosides [21], and adenosine triphosphate [22]. Until now, these aptasensors mainly aimed application in clinical diagnostics or served as model systems. For example, an optical aptasensor based on fluorescence quenching was developed for the detection of cocaine in serum [23], while a sensor based on cyclic voltametry (CV) and square wave voltametry (SWV) for the detection of 17β-estradiol in buffer [24] served as model system. But there are just a few aptasensors for environmental application. Especially for the detection of pharmaceutical residues in ground and drinking water, research studies are needed.

Doxorubicin and daunorubicin are also among the small molecules. In 2008, Wochner et al. selected and characterized highly specific and highly affine DNA aptamers for daunorubicin. The specific aptamer 10.10 displayed a slightly higher affinity for doxorubicin [25]. We used a truncated version of this aptamer in this study. Our aim was to develop an aptasensors for the detection of doxorubicin by electrochemical impedance spectroscopy (EIS). EIS is a fast, label-free technique for measuring the properties of electrode surfaces and bulk electrolytes. A significant advantage of this method is the non-destructive and label-free measurement of biological systems in their natural environment.

In this work, we present the development of a biosensor for the detection of doxorubicin using a specific daunorubicin-binding aptamer as biological recognition element. The thiol-modified aptamer was immobilized on gold electrodes by self-assembly, and binding of doxorubicin to the immobilized aptamer was measured in a three-electrode cell (Fig. 1a), in buffer solution containing ferri-/ferrocyanide as redox mediator. The interaction between the aptamers immobilized on gold and doxorubicin inhibits electron transfer between the electrode and ferro-/ferricyanide ($[Fe(CN)_6]^{3+/4+}$) in solution (Fig. 1b), which leads to an increase in impedance spectra.

Materials and methods

Reagents

The daunorubicin-binding aptamer (DRN-aptamer) applied in the current study is a 60 nucleotide-long truncated version of the 80 nucleotide-long aptamer selected by Wochner et al. [25]. Additionally, it was modified with C_6-spacer and thiol at the 5′ end: HS - C_6 - 5′- GGG AAT TCG AGC TCG GTA CCA TCT GTG TAA GGG GTA AGG GGT GGG GGT GGG TAC GTC TAG-3′. The spacer was included to increase distance between electrode surface and binding site for proper folding of the aptamer. A pool of randomized oligonucleotides (58 nt) was used as negative control (=DNA-pool): 5' ATA CCA GCT TAT TCA ATT NNN NNN NNN NNN NNN NNN NNN NNN NNN NNN NNN NNN N-3′ - C_6 - SH. It was synthesized by Microsynth AG (Balgach, Switzerland), modified with C_6-spacer and a thiol at the 3′ end, and purified with PAGE. 6-Mercapto-1-hexanol (MCH, 99%) was acquired from Sigma-Aldrich Chemie GmbH (Taufkirchen, Germany). Potassiumhexacyanoferrate (II) and (III) ($K_{3/4}[Fe(CN)_6]$) were purchased from Merck Chemicals GmbH (Darmstadt, Germany). Tris-(2-carboxyethyl)phosphinehydrochloride (TCEP) was purchased from Carl Roth GmbH+Co.KG (Karlsruhe, Germany). All reagents were of analytical grade and used without further purification. All working solutions were prepared in water purified with a Milli-Q Type-1-system (EMD Millipore Corporation, Billerica, MA, USA; 18 MΩ*cm). For aptamer experiments, the binding buffer (BB), consisting of 20 mM Tris/base, 140 mM NaCl, 5 mM KCl, 1 mM $CaCl_2$, 1 mM $MgCl_2$ (pH adjusted to 7.4 with HCl), was autoclaved and sterile-filtered before further usage.

The anthracyclines doxorubicin and daunorubicin (as hydrochlorides purchased from Sigma-Aldrich Chemie GmbH, Taufkirchen, Germany) were directly dissolved and diluted in BB. For electrochemical measurements 2 mM of $K_{3/4}[Fe(CN)_6]$ (equimolar) were added to BB (=FeBB).

Preparation of electrodes

The thiol-modified DRN-aptamer was preconditioned with TCEP (200 μM/μM thiol) for 20 min at room temperature to reduce disulfides and then heated to 95 °C for 5 min in BB to enable proper folding and immediately chilled on ice for 5 min. The gold electrodes and gold covered quartz crystals were exposed to UV light for 5 min and subsequently

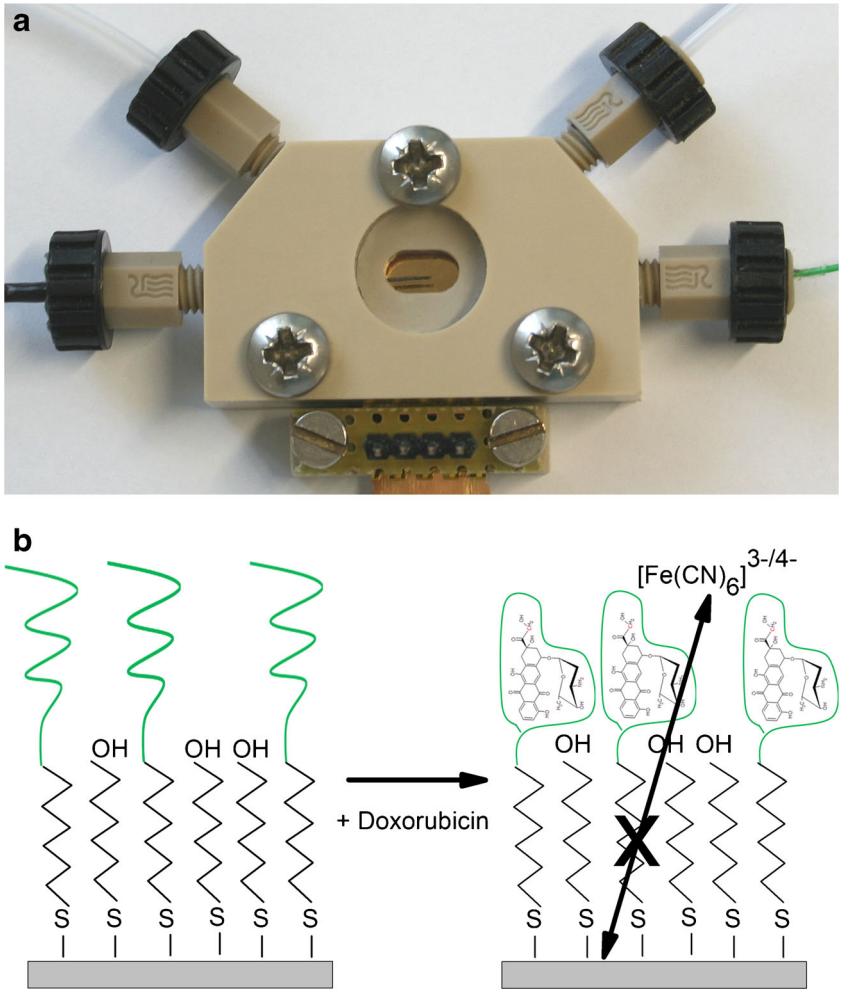

Fig. 1 **(a)** Flow-through measurement chamber with three electrode-system; **(b)** immobilization and measurement principle – upon binding of doxorubicin to the immobilized aptamer, the impedance increases due to the hindrance of electron transfer between electrode, and ferri-/ferrocyanide $[Fe(CN)_6]^{3-/4-}$

incubated in hot alkaline piranha solution (5:1:1 water:NH_3:H_2O_2; CAUTION: this acidic mixture reacts violently with any organic materials and must be handled with care!) for 5 min in an ultrasonic bath. After rigorous rinsing with ultrapure water, the electrodes were dried in nitrogen, immediately covered by 0.5 μM thiol-modified DRN-aptamer and 1.5 μM MCH in BB and incubated at room temperature overnight. Next day the surface was washed extensively with BB and blocked with 1 mM MCH for 30 min to fill the gaps occurring during the arrangement to an ordered monolayer, followed by another wash with BB. The modified electrodes were stored in BB until usage.

QCM measurements

To check the immobilization of the aptamer, a quartz crystal microbalance (QCM, Q-Sense Analyzer E4; Biolin Scientific Holding AB, Stockholm, Sweden) was used. The gold covered quartz crystal chips (QSX301, resonance frequency 4.95 MHz ± 50 kHz, Biolin Scientific) were cleaned as described above and then inserted into the flow module QFM401. For measurements, a baseline in BB was achieved, and then the chamber was filled with a solution of 0.5 μM DRN-aptamer and 1.5 μM MCH in BB and incubated overnight while the frequency change was continuously measured. A constant temperature of 21 °C was ensured. Next day the crystal was blocked with 1 mM MCH for 30 min and washed with BB. The relative frequency change – difference of frequency change measured in BB before and after incubation with aptamer – was used to determine the mass change by the Sauerbrey equation [26]. In that way, most of the influences of viscosity and density of the fluids were compensated.

EIS measurements

Electrochemical impedance spectroscopy (EIS) measurements were performed using the SP-300 potentiostat/galvanostat with impedance analyzer (Bio-Logic Science Instruments SAS, Claix, France). A flow-through chamber (Fig. 1a) made of polyether-ether-ketone (PEEK) was designed and manufactured. Flow-through was realized by a peristaltic pump and a Teflon tube of 0.5 mm inner diameter.

The fluid chamber with a volume of 100 μL was covered with glass. It consists of a three-electrode system with a working electrode cut from gold-coated test slides [TA134-(Ti/Au); EMF Corporation, Ithaca, NY, USA], a Pt-black wire as counter electrode, and Ag/AgCl reference electrode (E255 B, Science Products GmbH, Hofheim, Germany). The electrochemical active area (A_{true}) of the working electrode was determined by cyclic voltammetry in 0.5 M H_2SO_4 with 100 mV/s from 0 to 1.5 V. By integration of the reduction peak at ~750 mV, the required charge for reduction of a gold oxide monolayer is obtained (= 0.26 μC). Divided by the theoretical value, 482 μC/cm^2 [27], results in $A_{true} = 0.54 \pm 0.02$ cm^2. The geometric surface area, A_{geo}, was 0.246 cm^2 and thus, the roughness factor $R = A_{true}/A_{geo}$ was 2.2. The flow-through chamber and the solutions were kept in a temperature cabinet at 21 °C while the pump and impedance analyzer are positioned on the outside.

EIS measurements were performed with the aptamer-modified gold electrode mounted in the flow-through measurement chamber (Fig. 1a). Different concentrations of doxorubicin (4 to 1000 nM), 6 mL of each, were pumped with 50 μL/s through the chamber and incubated for 5 min while flow-through was stopped. Then 6 mL FeBB was pumped with 50 μL/s through the system. Finally, the impedance was measured from 1 Hz to 200 kHz with 7 logarithmic spaced frequencies per decade. The sinusoidal alternating voltage with an amplitude of 10 mV was applied at the equilibrium potential of ferri-/ferrocyanide (Eeq = ~140 mV). Fitting was performed with the simplex algorithm implemented in EC-Lab® software (v11.00, Bio-Logic Science Instruments SAS, Claix, France). The same procedure was applied to negative controls, chloramphenicol and tetracycline, of which 500 nM were used.

Results

Aptamer immobilization

The immobilization of the aptamer was performed as described in above. To increase the aptamer density, we adapted the co-immobilization procedure from Keighley et al. [28]. According to them, mercaptohexanol (MCH) avoids sticking of aptamers to the electrode surface. Standing upright, the aptamers occupy less space and thus enable higher densities. Quartz crystal microbalance (QCM) measurements were used to investigate and quantify the immobilization of the aptamer. Figure 2 shows the mass change upon immobilization of the DRN-aptamer in comparison to a mercaptohexanol (MCH) monolayer.

In the co-immobilization of the DRN-aptamer with MCH, a mass change of 500 ng/cm^2 was detected (Fig. 2). In comparison, a significantly lower mass change of 90 ng/cm^2 was observed after immobilization of a MCH monolayer.

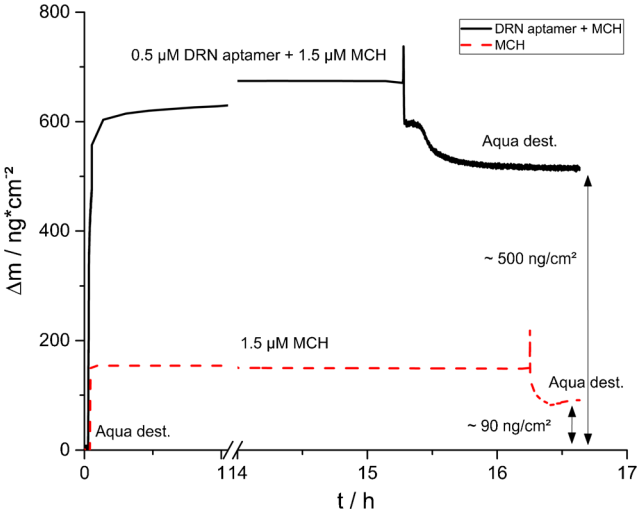

Fig. 2 QCM measurement: mass change Δm versus time of gold covered quartz crystals incubated with DRN aptamer (black solid line) or mercaptohexanol (MCH; red dashed line) measured in BB and water

To quantify the mass change of aptamer immobilization, the mass change for a MCH monolayer was subtracted from the detected mass change of DRN-aptamer-modified electrodes. The average mass increase of immobilized aptamers was 408 ± 76 ng/cm^2. This correlates to $1.3 \cdot 10^{13} \pm 2.4 \cdot 10^{12}$ molecules/cm^2.

Furthermore, the change in impedance during the immobilization of the DRN-aptamer was investigated by means of electrochemical impedance spectroscopy (EIS). Figure 3 shows the impedance spectrum of a DRN-aptamer-modified gold electrode (red plus). For comparison, the impedance spectra of a bare (black cross) and a MCH-coated gold electrode (blue triangles) are shown.

To extract the relevant parameters (Table 1), the impedance spectra were fitted to the modified Randles circuit (Fig. 3), where R_s is the solution resistance, CPE is the constant phase element for the double layer at the electrode surface, R_{ct} is the charge-transfer resistance due to the interaction of ferri-/ferrocyanide with the electrode, and W is the Warburg impedance representing the diffusion of all ions to the electrode surface.

The solution resistance R_s was independent of the coating type since this remained at a constant value of approximately 29.6 ± 0.4 Ω*cm^2. However, the electron transfer resistance R_{ct} changed depending on the coating. A bare gold electrode exhibited the lowest R_{ct} value of 70 ± 17 Ω*cm^2, whereas a gold electrode coated with a MCH monolayer had the highest R_{ct} value of 306 ± 52 Ω*cm^2. This was due to the fact that alkanethiols on a gold surface build a uniform self-assembly monolayer that constrains the electron transfer between the solution and the electrode. The R_{ct} of the gold electrode coated with a mixture of MCH and DRN aptamer was 199 ± 76 Ω*cm^2, which lies in between the bare and the MCH-coated gold

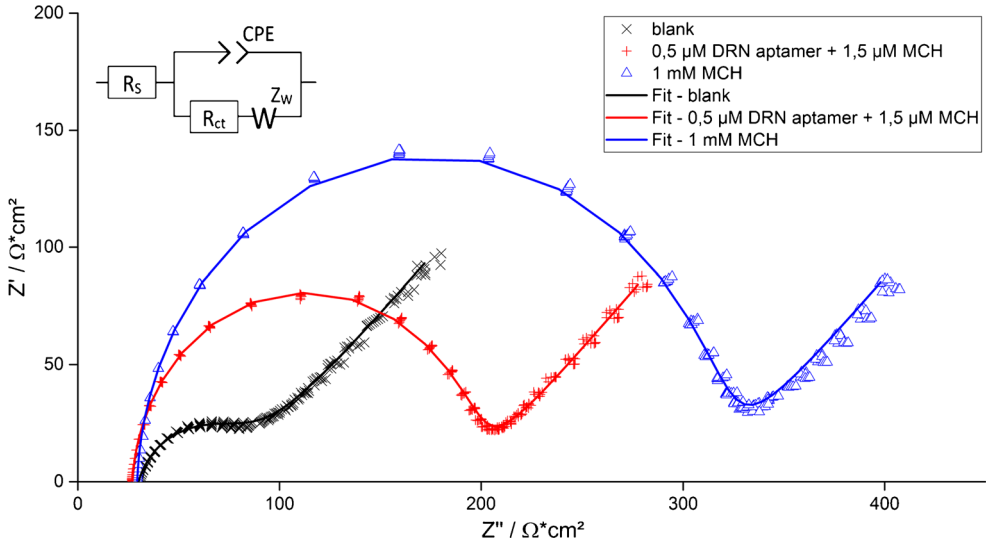

Fig. 3 Nyquist plot of a blank (black cross) electrode, a DRN-aptamer-modified electrode (red plus), and MCH-modified electrode (blue triangles) measured in FeBB – the colored solid lines represent the fits to the equivalent circuit

electrode. Owing to the aptamers, the alkanthiol monolayer contains "imperfections", thus, the electron transfer is higher than for the MCH monolayer. We successfully detected the immobilization of the DRN-aptamers on gold electrodes.

Detection of doxorubicin by impedance spectroscopy

The gold electrodes modified with aptamer were mounted in the impedance flow-through chamber and exposed to different concentrations of doxorubicin (4–1000 nM). Every doxorubicin concentration was measured on three different electrodes to determine reproducibility.

Figure 4a shows the Nyquist plot of a DRN-aptamer modified electrode and the same after exposure to 8, 62, and 125 nM doxorubicin. After incubation with doxorubicin, the impedance increased proportional to the rising concentration of doxorubicin. To extract the charge-transfer resistance R_{ct}, the impedance spectra were fitted to the modified Randles circuit. In Fig. 4b, the change of R_{ct} values [$=R_{ct}(sample)$-$R_{ct}(baseline)$] is plotted versus the doxorubicin concentration. The curve was fitted to the Hill Eq. 1:

$$Hill\ equation: \qquad \Delta R_{ct} = \frac{c^h}{K_D^h + c^h} \tag{1}$$

where h is the Hill coefficient, c denotes ligand concentration, and K_D is a dissociation constant.

The binding curve was a nonlinear sigmoidal function and starts at ΔR_{ct} = 6 Ω*cm^2 attributable to the unspecific signal of the binding buffer. An apparent K_D value of 64.4 ± 3.5 nM and an h of 3.4 ± 1.0 were obtained. The limit of detection (LoD) is defined as the lowest target concentration at which signal is higher than 3*σ. Using the approximated Hill equation, a LoD of 28.3 nM was determined.

Investigation of selectivity

In the development of biosensors, nonspecific binding is a known problem. Therefore, we investigated the binding of doxorubicin to different modified surfaces. Every experiment was measured on three different electrodes. The unspecific signals were lower than the specific signals (Fig. 5a). Furthermore, we investigated binding of structurally and functionally similar drugs, such as chloramphenicol and tetracycline to DRN-aptamer-modified gold electrodes (Fig. 5b). The aptamer showed no cross-reactivity to these molecules.

Discussion

Aptamers have already been selected against a wide variety of targets and used as biomimetic receptors in aptasensors. The targets can range from small molecules to large proteins [30]. So far, especially the detection of large proteins, e.g., thrombin [31–33] and immunoglobulin [34, 35] were investigated. Thus, aptamers against protein targets have been described comprehensively, but the range of small molecules still has great potential.

The detection of small target molecules can be difficult since molecular weight and interaction sites are low and therefore many detection methods are not applicable. Doxorubicin and daunorubicin are also among the small molecules, the detection of which are important for diagnostic and environmental-analytical applications.

In this work, an impedimetric aptasensor against doxorubicin was characterized. For this purpose, a microfluidic measuring system with a three-electrode arrangement was first developed. The quartz crystal microbalance allowed the establishment of the co-immobilization of the DRN-aptamer with mercaptohexanol on a gold surface. This immobilization

Table 1 Fit parameters of different modified electrodes; R_s = solution resistance, C_{eff} = effective capacitance (calculated by [29]), R_{ct} = charge-transfer resistance and W = Warburg impedance (from three different electrodes)

	Bare	0.5 μM DRN-aptamer + 1.5 μM MCH	1 mM MCH
R_S / Ω*cm^2	30.1 ± 0.2	29.4 ± 0.9	29.3 ± 0.2
R_{ct} / Ω*cm^2	70.4 ± 16.9	198.8 ± 76.1	305.7 ± 52.4
W / Ω*s$^{-1/2}$*cm^{-2}	295.8 ± 27.8	490 ± 75.1	505.9 ± 45.6
C_{eff} / μF*cm^{-2}	17.7 ± 1.3	4.8 ± 0.9	3.4 ± 0.9

strategy has already been described and successfully applied [28]. An average mass change of 408 ng/cm^2 ± 76 ng/cm^2 corresponding to the number of the immobilized DRN-aptamer of 1.3*10^{13} ± 2.4*10^{12} aptamer molecules/cm^2 was detected. The immobilization of the thiol-modified DRN-aptamer on gold via mercaptide bonds was successfully carried out and demonstrated. For measuring the stability of the system, the impedance behavior of modified gold electrodes was investigated over a period of 60 h. The change of the charge-transfer resistance with time was 6 ± 3 Ω*cm^2*h^{-1}. This change is not significant due to the short measurement time of 10 min.

By means of electrochemical impedance spectroscopy, the detection of the aptamer-target binding took place over a broad concentration range from 4 up to 1000 nM. Already from a concentration of 125 nM, the aptamer-doxorubicin-binding reached its saturation. The concentration range used was based on the results obtained by Wochner et al. (2008) by means of surface plasmon resonance spectroscopy (SPR) of the specific 80 nucleotide-long aptamer 10.10 and its two

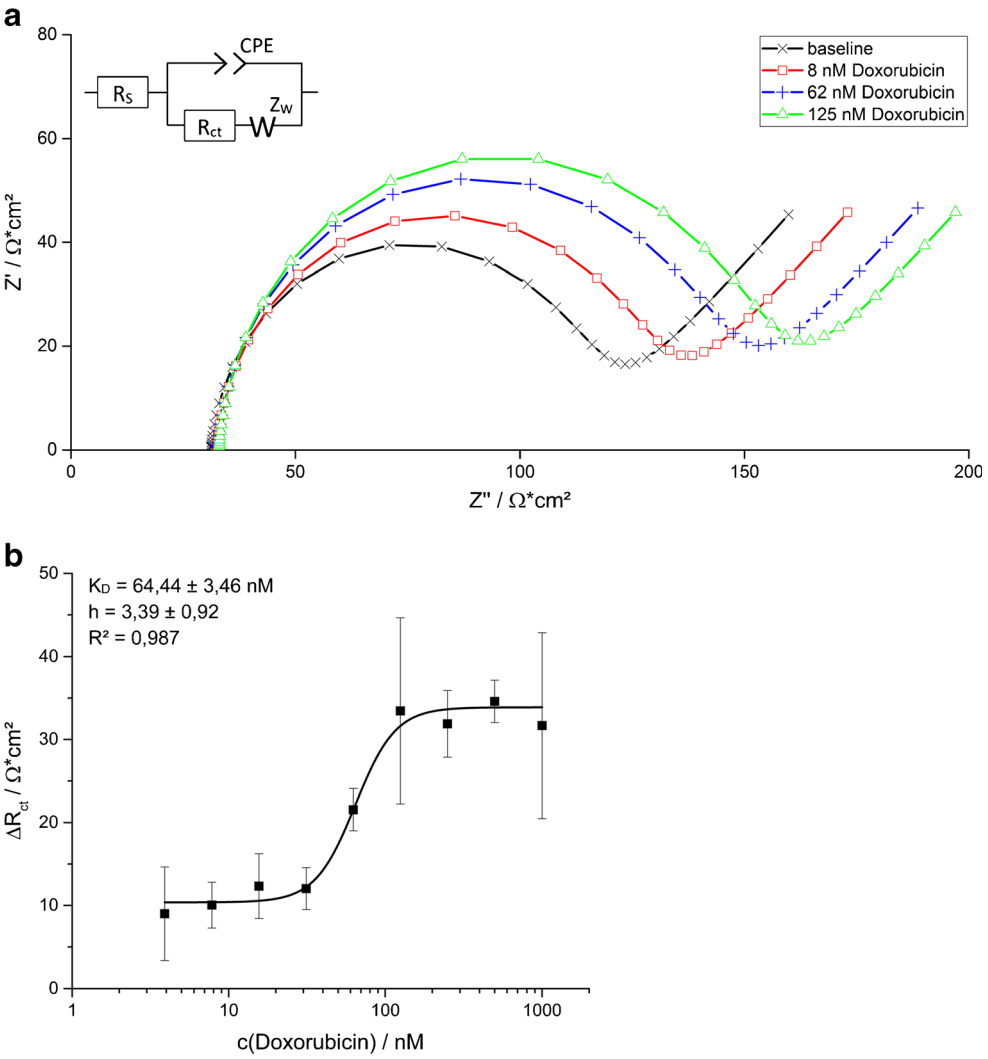

Fig. 4 **(a)** Nyquist plot of a DRN-aptamer-modified electrode (black cross) and the same after exposure to 8 nM (red squares), 62 nM (blue pluses), and 125 nM doxorubicin (green triangles) measured in FeBB – the fits to the equivalent circuit are shown as lines; **(b)** binding curve of doxorubicin to DRN-aptamer-modified electrodes; concentration of doxorubicin versus change of charge-transfer resistance R_{ct}

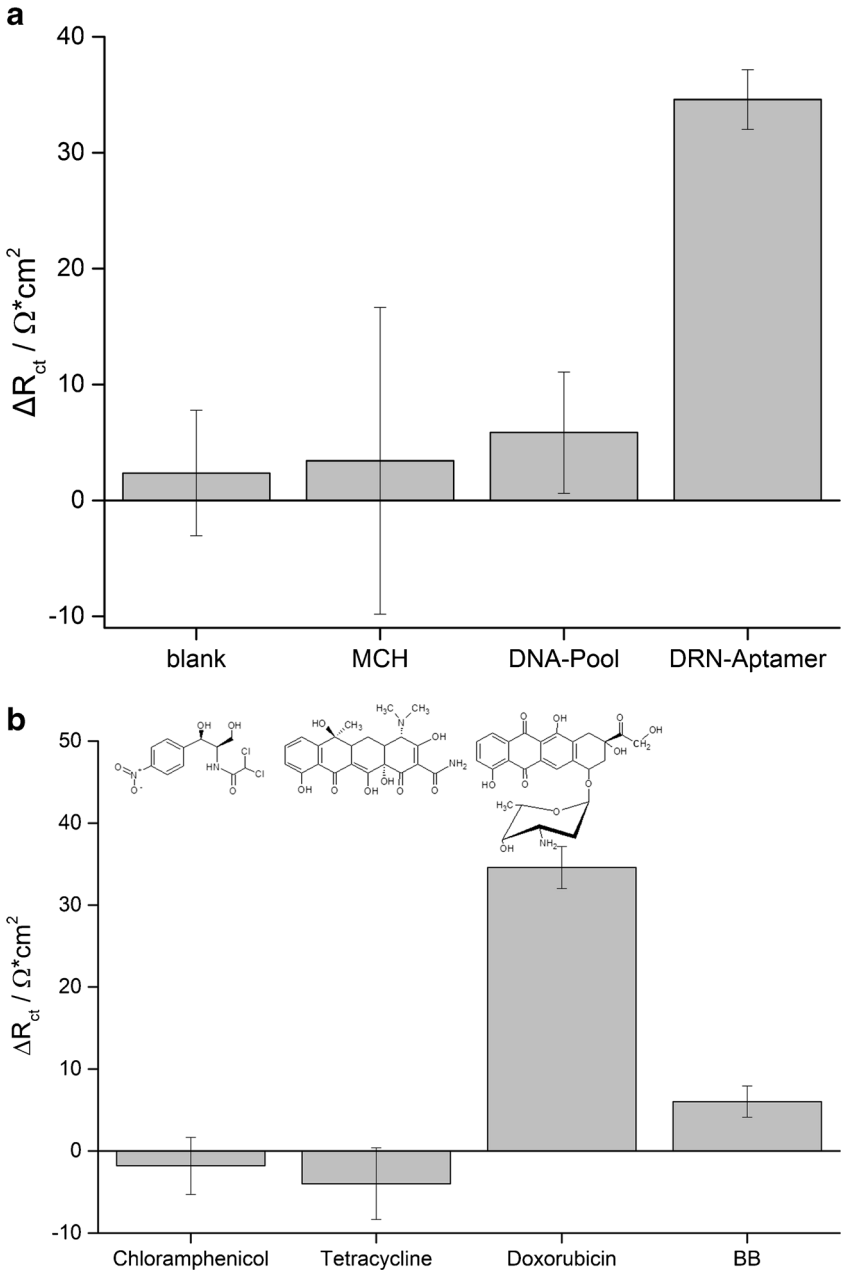

Fig. 5 Illustration of the unspecific signals (extracted *ΔRct*) of (**a**) 0.5 μM doxorubicin on blank electrodes and electrodes modified with a DNA-pool, MCH, and DRN-aptamer; (**b**) 0.5 μM chloramphenicol and 0.5 μM tetracycline as well as 0.5 μM doxorubicin and BB on DRN-aptamer-modified electrodes

truncated versions 10.10v and 10.10q, selected for detection of daunorubicin (see Table 2). In comparison to the full-length aptamer 10.10, the truncated 41 nucleotide-long version 10.10v has shown an about 10-fold weaker affinity to daunorubicin, whereas the truncated 23 nucleotide-long version 10.10q lost its affinity completely to daunorubicin [25]. The truncated 60 nucleotide-long version of the aptamer 10.10, used in this study, has shown a similar affinity to daunorubicin and doxorubicin as the specific daunorubicin aptamer 10.10 in later investigations (data not published yet). These results suggest that an optimization of the specific daunorubicin aptamer 10.10 by intensive truncation and mutation, for instance by a so-called Doped-SELEX [36] against both doxorubicin and daunorubicin, could improve effectively the affinity and specificity of this aptamer and thus increase the sensitivity of the developed aptasensor in this study against both anthracycline derivates.

The signal change increased with increasing doxorubicin concentration; thus the concentration-dependent aptamer-target binding was successfully detected by the means of impedance spectroscopy. Similar results were obtained for daunorubicin (data not shown). The anthracyclines also have the ability to intercalate in dsDNA at 5 μM [37] and ssDNA at 44 μM [37, 38]. This fact was not attributable to the specific binding to the DRN-aptamer, since the determined K_D of 64 nM and the signal for the DNA-pool were significantly lower.

Table 2 Apparent affinities K_D determined from DRN-aptamers with different nucleotide length [25]

Aptamer	Reference	Nucleotids	Sequence	K_D / nM	Principle
10.10q	[25]	23	AGGGGTAAGGGGTGGGGGTGGGT	-	Aptamer binds to immobilized daunorubicin
10.10v	[25]	41	ACC ATCTGTGTA AGGGGTAAGGGGTGGGGGTGGGT ACGTCT	272	Aptamer binds to immobilized daunorubicin
DRN	This work	60	GGGAATTCGAGCTCGGTACC ATCTGTGTA AGGGGTAAGGGGTGGGGGTGGGT ACGTCTAG	64	Doxorubicin binds to the immobilized aptamer
10.10	[25]	80	GGGAATTCGAGCTCGGTACC ATCTGTGTA AGGGGTAAGGGGTGGGGGTGGGT ACGTCTAG CTGCAGGCATGCAAGCTTGG	20	Aptamer binds to immobilized daunorubicin

The determined Hill coefficient h of 3.4 ± 1.0 indicates positive cooperativity, meaning that more than one interaction binding site is available [39]. However, the Hill coefficient does not give information on the total number of binding sites. No previous analysis of avidity effects for the daunorubicin-binding aptamers was performed. Thus, no comparison is possible. But positive cooperativity can also be found in other aptasensors [40–42].

The determined LoD of our developed aptasensor for doxorubicin is with 28.3 nM above previously reached detection limits of electrochemical aptasensors for the detection of small molecules, as, e.g., adenosine triphosphate with 5.6 nM [43], ethanolamine with 80 pM [44], and aflatoxin M1 with 3.5 pM [45]. It is lower than the LoD for doxorubicin previously reported by Erdem et al. (128 nM) [15]. Still, it is not sensitive enough to detect the concentrations of doxorubicin in clinical waste water (0.48 to 2.48 nM) [4]. Thus, optimization is necessary. Besides the methods mentioned above, the sensitivity of the aptasensor could be improved by the use of a combination of different aptamers for doxorubicin or the optimization of the spacer. Using these strategies, Lao et al. improved the detection of thrombin from nanomolar to picomolar [46].

The advantages of the developed electrochemical microfluidic aptasensor are low cost sensor surfaces, automation of the measurement procedure, and rapid results, which are obtained within 10 min.

In addition, the cross-reactivity of the DRN-aptamer and the nonspecific binding of doxorubicin on the sensor surface were investigated. The nonspecific signals of doxorubicin to gold (ΔR_{ct} = 2.4 Ω*cm^2), mercaptohexanol (ΔR_{ct} = 3.4 Ω*cm^2), and DNA-pool (ΔR_{ct} = 5.9 Ω*cm^2) were significantly below the specific signals of doxorubicin to the DRN-aptamer (ΔR_{ct} = 34.6 Ω*cm^2). The DRN-aptamer did not interfere with the structurally similar substances chloramphenicol and tetracycline. A similar result was achieved by Wochner et al. [25] and SPR. The low nonspecific signals could be based on the random error of the system. Repeated measurements of an aptamer-modified electrode in FeBB resulted in a standard variation σ of 4.88 Ω*cm^2. The electrochemical impedance is strongly temperature-dependent. The used temperature cabinet might not avoid temperature gradients within the chamber. By using temperature measurement directly in the flow through chamber, the error could be reduced.

Further studies are necessary to check the applicability of the biosensor. For analysis of real samples, such as drinking water, attention should be paid to the ion concentration. According to Wochner, besides the nature of the cations, mainly the ionic strength influences the binding of the aptamer to its target [47]. Necessary ions may be added to the sample.

The 60-nucleotide-long daunorubicin aptamer used, as already mentioned, had the following sequence: HS - C_6 - 5'-GGG AAT TCG AGC TCG GTA CCA TCT GTG TAA GGG GTA AGG GGT GGG GGT GGG TAC GTC TAG-3′. The underlined nucleotides determine the guanine-rich region. Owing to the high number of guanine, the aptamer is able to form G-quadruplexes. G-quadruplexes are multi-stranded structures that are formed and stabilized by vertical stacking of guanine tetrads by hydrogen bonds [48]. According to Wochner et al., the aptamer was shortened to 41 nucleotides, but the K_D value increased to 272 nM compared with a K_D value of 20 nM for the 80-nt-long DRN aptamer. In the case of shortening to the G-rich region (23 nucleotides), no significant binding affinity could be detected at the SPR [25]. However, the information obtained here is not sufficient to fully understand the aptamer–target bond. For an accurate structure elucidation of the aptamer–target complex, further investigations, such

as, e.g., CD spectroscopy and X-ray crystallography have to follow. The impedimetric aptasensor developed in this work provides a rapid, simple, and nondestructive analysis method for the detection of doxorubicin and daunorubicin. With this method, the detection of the two anthracyclines in the mid-nanomolar range was possible. This study also aims to contribute to the understanding of the detection of small molecules with aptamers.

Conclusions

The contamination of drinking water and groundwater with medicinal residues represents a growing environmental problem, so that the monitoring of water contamination plays a more important role. For this reason, steps toward an aptamer-based biosensor for the detection of the anthracycline doxorubicin were done.

The daunorubicin-aptamer was successfully immobilized on gold electrodes. Using the co-immobilization method, a density of $1.3*10^{13} \pm 2.4*10^{12}$ DNA molecules/cm^2 was achieved.

Detecting the binding of small molecules as doxorubicin (~580 g/mol) to the DRN-aptamer can be difficult due to low weight, small size, and few interaction sites. By the use of electrochemical impedance spectroscopy, doxorubicin was successfully detected by the decrease in electron transfer. Increasing concentrations from 4 to 1000 nM resulted in an increasing signal. In comparison, 500 nM of tetracycline and chloramphenicol, structurally similar molecules, gave signals below the background signal of the applied binding buffer. This confirmed the high specificity of the aptamer. From the binding curve a dissociation constant K_D of 64 nM and a detection limit LoD of 28.3 nM were determined. The aptamer shows a high sensitivity towards doxorubicin that proves the applicability of the aptamer for biosensor purposes. The reproducibility was in an acceptable range for the number of repetitions performed, as the standard deviation was 5 Ω*cm^2 for all measurements. For the detection of doxorubicin in residual water, our developed sensor will need further optimization.

In summary, we showed the proof of concept of an impedimetric aptasensor for the detection of doxorubicin in the mid-nanomolar range. Owing to the combination of aptamers and electrochemical impedance spectroscopy, our developed sensor unites rapid detection and easy automation of the measurement procedure with low cost and high specificity. Furthermore, due to the simplicity of the immobilization and the measurement principle, this concept can be transferred to other aptamers and used for the detection of multiple analytes.

Acknowledgements The authors gratefully acknowledge the Federal Ministry of Economic Affairs and Energy within the framework of the AiF-ZIM-program for supporting this project under grant nos. ZF4019603MD6 and ZF4086507MD6.

Compliance with ethical standards

Conflict of interest The authors declare no conflict of interest.

References

1. Rahman A, Goodman A, Foo W, Harvey J, Smith FP, Schein PS. Clinical pharmacology of daunorubicin in Phase I patients with solid tumors: development of an analytical methodology for daunorubicin and its metabolites. Semin Oncol. 1984;11(4):36–44.
2. de los Santos-Alvarez N, Lobo-Castanon MJ, Miranda-Ordieres AJ, Tunon-Blanco P (2008) Aptamers as recognition elements for label-free analytical devices. TrAC Trends Anal Chem 27(5):437-446
3. Hanna AD, Lam A, Tham S, Dulhunty AF, Beard NA. Adverse effects of doxorubicin and its metabolic product on cardiac RyR2 and SERCA2A. Mol Pharmacol. 2014;86(4):438–49.
4. Mahnik SN, Lenz K, Weissenbacher N, Mader RM, Fuerhacker M. Fate of 5-fluorouracil, doxorubicin, epirubicin, and daunorubicin in hospital wastewater and their elimination by activated sludge and treatment in a membrane-bio-reactor system. Chemosphere. 2007;66, 30(1):–37.
5. Chisvert A, Sisternes J, Balaguer Á, Salvador A. A gas chromatography–mass spectrometric method to determine skin-whitening agents in cosmetic products. Talanta. 2010;81(1):530–6.
6. Diallo S, Lecanu L, Greeson J, Papadopoulos V. A capillary gas chromatography/mass spectrometric method for the quantification of hydroxysteroids in human plasma. Analytical Biochemistry. 2004;324(1):123–30.
7. Kaushik D, Bansal G. Characterization of degradation products of idarubicin through LC-UV, MSn, and LC-MS-TOF studies. J Pharmaceut Biomedi Anal. 2013;85:123–31.
8. Fogli S, Danesi R, Innocenti F, Di Paolo A, Bocci G, Barbara C, Del Tacca M. An improved HPLC method for therapeutic drug monitoring of daunorubicin, idarubicin, doxorubicin, epirubicin, and their 13-dihydro metabolites in human plasma. Ther Drug Monit. 1999;21(3):367–75.
9. Chin DL, Lum BL, Sikic BI. Rapid determination of PEGylated liposomal doxorubicin and its major metabolite in human plasma by ultraviolet-visible high-performance liquid chromatography. J Chromatogr B Anal Technol Biomedi Life Sci. 2002;779(2):259–69.
10. Hassan HNA, Barsoum BN, Habib IHI. Simultaneous spectrophotometric determination of rutin, quercetin, and ascorbic acid in drugs using a Kalman filter approach. J Pharmaceut Biomed Anal. 1999;20(1):315–20.
11. Zhang F, Du Y, Ye B, Li P. Study on the interaction between the chiral drug of propranolol and α1-acid glycoprotein by fluorescence spectrophotometry. J Photochem Photobiol B Biology. 2007;86(3):246–51.
12. Sun S, Huang X, Ma M, Qiu N, Cai Z, Luo Z, Alies NP. Systematic evaluation of avidin–biotin interaction by fluorescence spectrophotometry. Spectrochim Acta Part A Mol Biomol Spectrosc. 2012;89:99–104.
13. Yang X, Gao H, Qian F, Zhao C, Liao X. Internal standard method for the measurement of doxorubicin and daunorubicin by capillary electrophoresis with in-column double optical-fiber LED-induced

fluorescence detection. J Parmaceut Biomed Anal. 2016;117:118–24.
14. Simeon N, Chatelut E, Canal P, Nertz M, Couderc F. Anthracycline analysis by capillary electrophoresis. Application to the analysis of daunorubicine in Kaposi sarcoma tumor. J Chromatogr A. 1999;853(1/2):449–54.
15. Erdem A, Karadeniz H, Caliskan A. Dendrimer modified graphite sensors for detection of anticancer drug daunorubicin by voltammetry and electrochemical impedance spectroscopy. Analyst. 2011;136(5):1041–5.
16. Strehlitz B, Reinemann C, Linkorn S, Stoltenburg R. Aptamers for pharmaceuticals and their application in environmental analytics. Bioanal Rev. 2012;4(1):1–30.
17. Velasco-Garcia MN, Missailidis S. New trends in aptamer-based electrochemical biosensors. Gene Ther Mol Biol. 2009;13(A):1–9.
18. Mann D, Reinemann C, Stoltenburg R, Strehlitz B. In vitro selection of DNA aptamers binding ethanolamine. Biochem Biophys Res Commun. 2005;338(4):1928–34.
19. Liang G, Man Y, Jin X, Pan L, Liu X. Aptamer-based biosensor for label-free detection of ethanolamine by electrochemical impedance spectroscopy. Anal Chim Acta. 2016;36:222–8.
20. Baker BR, Lai RY, Wood MS, Doctor EH, Heeger AJ, Plaxco KW. An electronic, aptamer-based small-molecule sensor for the rapid, label-free detection of cocaine in adulterated samples and biological fluids. J Am Chem Soc. 2006;128(10):3138–9.
21. Schoukroun-Barnes LR, Wagan S, White RJ. Enhancing the analytical performance of electrochemical RNA aptamer-based sensors for sensitive detection of aminoglycoside antibiotics. Anal Chem. 2014;86(2):1131–7.
22. White RJ, Rowe AA, Plaxco KW. Re-engineering aptamers to support reagentless, self-reporting electrochemical sensors. Analyst. 2010;135(3):589–94.
23. Stojanovic MN, de Prada P, Landry DW. Aptamer-based folding fluorescent sensor for cocaine. J Am Chem Soc. 2001;123(21):4928–31.
24. Kim YS, Jung HS, Matsuura T, Lee HY, Kawai T, Gu MB. Electrochemical detection of 17β-estradiol using DNA aptamer immobilized gold electrode chip. Biosens Bioelectron. 2007;22(11):2525–31.
25. Wochner A, Menger M, Orgel D, Cech B, Rimmele M, Erdmann VA, Glökler J. A DNA aptamer with high affinity and specificity for therapeutic anthracyclines. Anal Biochem. 2008;373(1):34–42.
26. Sauerbrey G. Verwendung von Schwingquarzen zur Wägung dünner Schichten und zur Mikrowägung. Zeitschrift Physik. 1959;155(2):206–22.
27. Oesch U, Janata J. Electrochemical study of gold electrodes with anodic oxide films, I. Formation and reduction behaviour of anodic oxides on gold. Electrochim Acta. 1983;28(9):1237–46.
28. Keighley SD, Li P, Estrela P, Migliorato P. Optimization of DNA immobilization on gold electrodes for label-free detection by electrochemical impedance spectroscopy. Biosens Bioelectron. 2008;23(8):1291–7.
29. Hirschorn B, Orazem ME, Tribollet B, Vivier V, Frateur I, Musiani M. Determination of effective capacitance and film thickness from constant-phase-element parameters. Electrochim Acta. 2010;55(21):6218–27.
30. Ilgu M, Nilsen-Hamilton M. Aptamers in analytics. Analyst. 2016;141(5):1551–68. https://doi.org/10.1039/c5an01824b .
31. Frense D, Kang S, Schieke K, Reich P, Barthel A, Pliquett U, Nacke T, Brian C, Beckmann D. Label-free impedimetric biosensor for thrombin using the thrombin-binding aptamer as receptor. J Phys: Conference Series. 2013;434:012091.
32. Li X, Shen L, Zhang D, Qi H, Gao Q, Ma F, Zhang C. Electrochemical impedance spectroscopy for study of aptamer–thrombin interfacial interactions. Biosens Bioelectron. 2008;23(11):1624–30.
33. Yang H, Ji J, Liu Y, Kong JL, Liu BH. An aptamer-based biosensor for sensitive thrombin detection. Electrochem Commun. 2009;11(1):38–40.
34. Yao CY, Qi YZ, Zhao YH, Xiang Y, Chen QH, Fu WL. Aptamer-based piezoelectric quartz crystal microbalance biosensor array for the quantification of IgE. Biosens Bioelectron. 2009;24(8):2499–503.
35. Papamichael KI, Kreuzer MP, Guilbault GG. Viability of allergy (IgE) detection using an alternative aptamer receptor and electrochemical means. Sensors Actuators B Chemical. 2007;121(1):178–86.
36. Ohuchi S, Mori Y, Nakamura Y. Evolution of an inhibitory RNA aptamer against T7 RNA polymerase. FEBS Open Bio. 2012;2:203–7.
37. Hynek D, Krejcova L, Zitka O, Adam V, Trnkova L, Sochor J. Electrochemical study of doxorubicin interaction with different sequences of single stranded oligonucleotides. Part I. Int J Electrochem Sc. 2012;7(1):13–33.
38. Gui-Fang C, Jie Z, Yong-Hua T, Pin-Gang H, Yu-Zhi F, Stiborová M, Eckschlager T, Hubálek J, Kizek R. Study on the interaction between antitumor drug daunomycin and DNA. Chin J Chem. 2005;23(5):576–80.
39. Cattoni DI, Chara O, Kaufman SB, González Flecha FL. Cooperativity in binding processes: new insights from phenomenological modeling. PLOS ONE. 2016;10(12):e0146043.
40. Swain MD, Octain J, Benson DE. Unimolecular, soluble semiconductor nanoparticle-based biosensors for thrombin using charge/electron transfer. Bioconj Chem. 2008;19(12):2520–6.
41. Urmann K, Reich P, Walter JG, Beckmann D, Segal E, Scheper T. Rapid and label-free detection of protein a by aptamer-tethered porous silicon nanostructures. J Biotechnol. 2017;257:171–7.
42. Blouin S, Lafontaine DA. A loop–loop interaction and a K-turn motif located in the lysine aptamer domain are important for the riboswitch gene regulation control. RNA. 2007;13(8):1256–67.
43. Shi P, Zhang Y, Yu Z, Zhang S. Label-free electrochemical detection of ATP based on amino-functionalized metal-organic framework. Sci Rep. 2017;7(1):–6500.
44. Liang G, Man Y, Jin X, Pan L, Liu X, Glökler J. Aptamer-based biosensor for label-free detection of ethanolamine by electrochemical impedance spectroscopy. Anal Chim Acta. 2016;936:222–8.
45. Istamboulié G, Paniel N, Zara L, Reguillo Granados L, Barthelmebs L, Noguer T. Development of an impedimetric aptasensor for the determination of aflatoxin M1 in milk. Talanta. 2016;146:464–9.
46. Lao Y-H, Peck K, Chen L-C. Enhancement of aptamer microarray sensitivity through spacer optimization and avidity effect. Anal Chem. 2009;81:1747–54.
47. Wochner A.. Selektion von Aptameren gegen Antibiotika und deren Einsatz in empfindlichen Assayformaten. Freie Universität Berlin. (2007).
48. Davis JT. 40 Jahre G-Quartetts: von 5′-GMP zur Molekularbiologie und Supramolekularen Chemie. Angew Chem. 2004;116(6):684–716.